New Phytologist

Research

Contrasting plant–soil–microbial feedbacks stabilize vegetation types and uncouple topsoil C and N stocks across a subarctic–alpine landscape

Carles Castaño[1], Sara Hallin[1], Dagmar Egelkraut[2], Björn D. Lindahl[3], Johan Olofsson[4] and Karina Engelbrecht Clemmensen[1]

[1]Department of Forest Mycology and Plant Pathology, Swedish University of Agricultural Sciences, SE-75007 Uppsala, Sweden; [2]Department of Biological Sciences, University of Bergen, 5006 Bergen, Norway; [3]Department of Soil and Environment, Swedish University of Agricultural Sciences, Uppsala SE-75007, Sweden; [4]Department of Ecology and Environmental Science, Umeå University, 90187 Umeå, Sweden

Author correspondence:
Carles Castaño
Email: carles.castanyo@slu.se

Received: *13 September 2022*
Accepted: *2 December 2022*

New Phytologist (2023) **238:** 2621–2633
doi: 10.1111/nph.18679

Key words: forest, fungal saprotrophs, grassland, heathland, mycorrhiza, N cycling, vegetation gradients.

Summary

- Global vegetation regimes vary in belowground carbon (C) and nitrogen (N) dynamics. However, disentangling large-scale climatic controls from the effects of intrinsic plant–soil–microbial feedbacks on belowground processes is challenging. In local gradients with similar pedo-climatic conditions, effects of plant–microbial feedbacks may be isolated from large-scale drivers.
- Across a subarctic–alpine mosaic of historic grazing fields and surrounding heath and birch forest, we evaluated whether vegetation-specific plant–microbial feedbacks involved contrasting N cycling characteristics and C and N stocks in the organic topsoil. We sequenced soil fungi, quantified functional genes within the inorganic N cycle, and measured ^{15}N natural abundance.
- In grassland soils, large N stocks and low C : N ratios associated with fungal saprotrophs, archaeal ammonia oxidizers, and bacteria capable of respiratory ammonification, indicating maintained inorganic N cycling a century after abandoned reindeer grazing. Toward forest and heath, increasing abundance of mycorrhizal fungi co-occurred with transition to organic N cycling. However, ectomycorrhizal fungal decomposers correlated with small soil N and C stocks in forest, while root-associated ascomycetes associated with small N but large C stocks in heath, uncoupling C and N storage across vegetation types.
- We propose that contrasting, positive plant–microbial feedbacks stabilize vegetation trajectories, resulting in diverging soil C : N ratios at the landscape scale.

Introduction

In terrestrial ecosystems, biogeochemical processes are driven by interactions among plants and soil microorganisms (Rousk & Bengtson, 2014; Bennett & Klironomos, 2019). Particularly, the plant rooting zone selects for microorganisms that may generate either negative or positive feedbacks to plant growth (Wardle, 2002; Van der Putten *et al.*, 2013). Negative feedbacks involve nutrient competition and pathogenic activities (Bell *et al.*, 2006; Mangan *et al.*, 2010), while positive feedbacks involve enhanced nutrient acquisition, for example, through mycorrhizal symbioses, and pathogen suppression (Bennett *et al.*, 2017; Lance *et al.*, 2020). While negative feedbacks may prevent dominance by single plant species (Mangan *et al.*, 2010), positive feedbacks may stabilize vegetation types (Van der Putten *et al.*, 2013). Plant–microbial feedbacks can involve modification of organic matter quality and nutrient cycling (Read & Perez-Moreno, 2003; Bennett & Klironomos, 2019). Particularly, abrupt transitions in mycorrhizal symbionts of dominant plants have been linked to shifting positive feedbacks between plants and microorganisms, generally related to carbon (C) and nitrogen (N) cycling (Egelkraut *et al.*, 2018b; Bennett & Klironomos, 2019; Clemmensen *et al.*, 2021). However, the belowground processes underpinning vegetation patterns are not well understood, although they may influence global soil C and N stocks (Averill *et al.*, 2014; Steidinger *et al.*, 2019).

Organic matter can be decomposed, and nutrient contents potentially released, by free-living, saprotrophic soil fungi, which through their filamentous growth and enzymatic capacities can overcome the spatial patchiness and recalcitrance of organic resources. However, almost all plants benefit from symbiotic associations with either arbuscular mycorrhizal (AM), ectomycorrhizal (ECM), or ericoid mycorrhizal (ERM) fungi to access soil nutrients (Smith & Read, 2008). A few ECM tree species from the genera *Betula*, *Pinus*, and *Picea* dominate Northern boreal and subarctic forests. These tree species are characterized by

© 2022 The Authors
New Phytologist © 2022 New Phytologist Foundation
This is an open access article under the terms of the Creative Commons Attribution-NonCommercial License, which permits use, distribution and reproduction in any medium, provided the original work is properly cited and is not used for commercial purposes.

relatively poor quality of both leaf and root litter, which together with a harsh climate lead to slow saprotrophic decomposition and low availability of N in the soil (Ward *et al.*, 2022). Trees may instead depend more on organic N mobilization, driven by associated ECM fungi (Phillips *et al.*, 2013; Lindahl & Tunlid, 2015). However, there is large variation among ECM fungi in how they interact with organic matter. ECM decomposers may oxidize organic matter via extracellular manganese peroxidase enzymes (Bödeker *et al.*, 2014) or Fenton chemistry (Rineau *et al.*, 2012; Op De Beeck *et al.*, 2018), while other ECM fungi lack genetic capabilities to decompose recalcitrant organic matter (Kohler *et al.*, 2015). Under low N availability, ECM decomposers may mine N bound in organic matter, increasing residual soil C : N ratios in organic horizons and decreasing total soil C and N stocks (Talbot *et al.*, 2008; Parker *et al.*, 2015; Clemmensen *et al.*, 2021; Lindahl *et al.*, 2021). In forests, this can promote positive feedbacks by providing trees exclusive access to otherwise unavailable soil N via their ECM fungal associates (Northup *et al.*, 1995; Bennett & Klironomos, 2019).

Much of the boreal and subarctic forest has an understory of ERM plant species belonging to the genera *Empetrum*, *Vaccinum*, and *Calluna*, and the same genera dominate boreal and arctic heathlands. Production of poor-quality litter by ericaceous plants (Cornwell *et al.*, 2008; Adamczyk *et al.*, 2016) and the recalcitrant nature of the mycelium of their associated ERM fungi (Fernandez & Kennedy, 2018; Adamczyk *et al.*, 2019; Tonjer *et al.*, 2021) may promote positive feedbacks, in this case by reducing decomposition (Fanin *et al.*, 2022), and thus N availability, to faster-growing plant species (Bennett & Klironomos, 2019). Ericoid mycorrhizal (ERM) fungi can contribute to plant N uptake (Hobbie & Hobbie, 2006; Hewitt *et al.*, 2015) and are genetically equipped for decomposition of a broad variety of organic compounds (Read & Perez-Moreno, 2003; Martino *et al.*, 2018). However, the larger C stocks in ERM systems relative to ECM systems (Hartley *et al.*, 2012; Clemmensen *et al.*, 2013, 2021; Parker *et al.*, 2015, 2021) suggest that ERM fungi use different mechanisms and/or are less efficient in accessing organic nutrient pools than ECM decomposers.

In Northern Europe, AM symbioses are mostly found in croplands or grasslands dominated by forbs and grasses that produce high-quality litter (Cornelissen *et al.*, 2001). As AM fungi lack the genes to access organic N (Smith & Read, 2008), saprotrophs in these systems drive soil organic matter decomposition and promote N mineralization (Phillips *et al.*, 2013; Lin *et al.*, 2017; Keller & Phillips, 2019). With increasing release of inorganic N species, bacterial communities involved in inorganic N cycling become more abundant, and the balance between different N cycling guilds further determine whether N is fixed from the atmosphere (via diazotrophy), retained (e.g. via dissimilatory nitrate reduction to ammonium, DNRA), or lost in gaseous or water-soluble forms (e.g. via denitrification or nitrification; Zhao *et al.*, 2017; Putz *et al.*, 2018).

It is uncertain whether links between ECM–AM mycorrhizal regimes and soil C : N ratios are driven by differences in soil N or C stocks, or both (Averill *et al.*, 2014; Zhu *et al.*, 2018). Further, the mechanisms that drive heathlands (Ward *et al.*, 2021), and potentially some grasslands (Stark *et al.*, 2019), to accumulate large soil organic stocks are not well established. At the global scale, mycorrhizal regimes covary with pedo-climatic conditions (Read, 1991; Steidinger *et al.*, 2019), which makes it difficult to establish causal relationships between the shifts in mycorrhizal types and soil characteristics. We therefore used a landscape-level mosaic of grassland, heathland, and forest vegetation patches, with limited confounding pedo-climatic variation, to investigate whether different plant–microbial feedbacks stabilize vegetation types while driving contrasting trajectories of soil C and N storage. The grasslands were historical reindeer grazing fields (milking grounds) surrounded by ericaceous heathlands and mountain birch forests in a subarctic–alpine ecotone in northern Sweden (Egelkraut *et al.*, 2018a). Analysis of historical aerial photographs indicated that the milking grounds are still stable despite abandonment over 100 yr ago, although some areas are slowly being colonized from the edges by the surrounding vegetation. We combined DNA-based characterization of soil microbial communities with biogeochemical analyses. We also analyzed natural abundances of stable N isotopes, which can indicate processes underlying variation in C and N stocks (Robinson, 2001; Hobbie & Högberg, 2012).

We hypothesized (H1) that the mosaic of heath, forest, and grassland (historic milking grounds) vegetation is stabilized by different plant–soil feedbacks involving different modes of microbial N cycling. Specifically, in grasslands, we expected grasses and forbs to associate with AM fungi and a high relative abundance of saprotrophic fungi to promote organic matter decomposition and N mineralization, leading to inorganic N cycling by bacteria and archaea. In forests, trees would associate with ECM fungi that promote organic N mining through decomposition of organic matter, and in heaths, dwarf shrubs and associated ERM fungi would promote organic N cycling but constrain decomposition by hampering saprotrophs. We further hypothesized (H2) that the contrasting plant–soil feedback mechanisms would have led to diverging long-term soil C and N stocks in grasslands, heaths, and forests. Thus, we expected uncoupled soil C and N storage across the vegetation mosaic; C stocks would be highest in heath, intermediary in forest, and lowest in grassland, while N stocks would be highest in grassland, intermediary in heath, and lowest in forest.

Materials and Methods

Study system and soil sampling

We used seven historical milking grounds and surrounding vegetation situated in the sub-alpine-to-alpine ecotone within a 2 × 2 km area between Staloluokta (67°19′5.1888″N, 16°41′51.1476″E) and Staddajåkkå (67°14′27.2364″N, 16°35′28.5252″E) in Badjelánnda National Park (NE Sweden; Supporting Information Fig. S1). Average yearly temperatures in the area have increased from −1.8 to 0.5°C between 1961 and 2014, and average yearly precipitation is 968 mm. Milking grounds are cultural remains of historical (*c.* 1350–1900 AD) Sami reindeer husbandry, in which reindeer were kept for milk production during summer months

© 2022 The Authors
New Phytologist © 2022 New Phytologist Foundation

14698137, 2023, 6, Downloaded from https://nph.onlinelibrary.wiley.com/doi/10.1111/nph.18679 by Swedish University Of Agricultural Sciences, Wiley Online Library on [28/07/2023]. See the Terms and Conditions (https://onlinelibrary.wiley.com/terms-and-conditions) on Wiley Online Library for rules of use; OA articles are governed by the applicable Creative Commons License

and the high grazing pressure, resulted in vegetation patches dominated by grasses and forbs (Egelkraut *et al.*, 2018a).

The milking grounds are surrounded by Arctic downy birch (*Betula pubescens* Ehrh) forest or heath vegetation (dominated by *Empetrum nigrum* and *Vaccinum* spp., Fig. S1). Near each milking ground ($n = 7$), control plots representing the same soil type, topology, and position in the landscape were selected previously to represent the vegetation type that most probably would have dominated the milking ground area without the historical grazing (Egelkraut *et al.*, 2018a). Five milking grounds were paired with heath vegetation controls ($n = 5$) and two with mature birch forest controls ($n = 2$; Fig. S1). Sampling plots of 5 × 10 m in the central part of each milking ground and in the paired heath and forest controls were set up for vegetation analyses in a previous study (Egelkraut *et al.*, 2018a). To facilitate studies of smaller-scale, plant–soil interactions, soil sampling plots of 0.5 × 0.5 m were established inside the vegetation plots. While these plots may have failed to cover spatial variation around larger trees, we prioritized to keep plot size equal across all vegetation types. Additional 0.5 × 0.5 m plots were set up along the outer circumference of each milking ground within zones that had been colonized by the surrounding vegetation between 1964 and 2008, as determined by comparisons of two sets of aerial photographs (Egelkraut *et al.*, 2018a). For this, historical outlines of the milking grounds were converted to line plots in a handheld GPS, which were inspected during fieldwork (Fig. S1). Recently colonized zones were categorized as either colonizing heath ($n = 7$; dominated by *Empetrum nigrum* L.) or colonizing forest ($n = 8$; dominated by *B. pubescens* saplings). In addition, 0.5 × 0.5 m plots were set up under the closest established *B. pubescens* tree (established tree) outside each of the milking grounds ($n = 6$, excluding one milking ground). These established trees were either solitary trees located close to the milking grounds, or they were on the edge of the closest forest and were therefore analyzed separately from the mature forest controls.

In July 2016, three soil cores including the litter layer and the complete organic horizon (the O-horizon; hereafter 'organic topsoil') were collected in each of the 35 plots, using a 3-cm diameter cylindrical steel corer with a sharpened edge. The fully organic topsoil, which was commonly 10–20 cm thick, rested on mostly shallow mineral soil or directly on bedrock. Thus, only organic topsoils were sampled quantitatively to their full depth and according to surface area (in total 21.2 cm^2 per plot), but sampling depth was variable across sampling points due to the variable thickness of the organic topsoil. Preserving soil stratification, the 105 soil cores were kept cool (at *c.* 10°C) in separate plastic bags for up to 3 d during transport and then frozen at −20°C until processed.

Sample preparation and carbon, nitrogen, and stable isotope analyses

The three soil cores from each plot were separated into the superficial litter layer (L, constituting on average 10 and 2.4% of the organic topsoil carbon and mass, respectively), the upper half of the humus layer (H1), and the lower half of the humus layer, including any humus-mineral soil transition, if present (H2). The mineral soil was otherwise not included in the study. Living roots, stems, and woody debris larger than 2 mm in diameter were removed (i.e. finer roots were left in the sample), and the samples from the same horizon were pooled within plots, resulting in a total of 35 plots × 3 horizons = 105 samples. The composite samples were weighed to obtain the total fresh weight of the organic topsoil per sampled area (based on the added area of the tree soil cores), and a subsample was weighed before and after freeze-drying to obtain water content for calculation of total soil dry mass per m^2. The freeze-dried samples were ground with a mortar and pestle to a fine powder. Organic content was determined by loss-on-ignition at 550°C for 6 h (to account for in-mixing of mineral soil in the otherwise organic samples), and samples were analyzed for total C and N content as well as $^{15}N : {}^{14}N$ isotopic ratios (Methods S1).

DNA extraction and quantitative PCR (qPCR) of marker genes

DNA was extracted from 150 mg (H1 and H2 horizons only; as we targeted root–microbial interactions, the root-free litter layer was not included in microbial analyses) of freeze-dried and milled soil using the NucleoSpin Soil kit (Macherey-Nagel, Düren, Germany). DNA concentration was measured on a Qubit Fluorometer (Life Technologies), and the extracts were diluted to 3 ng DNA μl^{-1} of which 2 µl (6 ng DNA) was used per PCR reaction of 20 µl. PCR inhibition was checked for all samples (Methods S1).

Total fungal and bacterial community sizes were evaluated by quantification of the fungal internal transcribed spacer region 2 (ITS2), using the primers fITS7 (Ihrmark *et al.*, 2012), ITS4 (White *et al.*, 1990) and ITS4arch (Sterkenburg *et al.*, 2015), and the V3 region of the bacterial 16S rRNA gene, using the primers 341F and 534R (López-Gutiérrez *et al.*, 2004), respectively. Genetic potential for ammonia oxidation was determined by quantification of *amoA* genes of ammonia-oxidizing archaea (AOA), using the primers crenamoA23F and crenamoA616R (Tourna *et al.*, 2008), and ammonia-oxidizing bacteria (AOB), using the primers AmoA1F and AmoA2R (Rotthauwe *et al.*, 1997). This process is a precursor of N loss as it results in the production of nitrate, a water-soluble and highly mobile N species, and further also fuels gaseous N losses through denitrification. Additionally, *nrfA* genes, involved in respiratory ammonification (a step in dissimilatory nitrate reduction to ammonium (DNRA)), were amplified using the primers NrfA2aw and NrfAR1 (Welsh *et al.*, 2014) to assess the genetic potential for internal retention of N in the system, and *nifH* genes were quantified using the primers Ueda19F (Ueda *et al.*, 1995) and R6 (Marusina *et al.*, 2001) to assess the genetic potential for diazotrophic N_2 fixation. Primer information, qPCR mix, cycling conditions, and amplification efficiencies are listed in Table S1. Detailed qPCR procedure is available in Methods S1.

Fungal community sequencing

Fungal communities were PCR-amplified in duplicates using the forward gITS7 (Ihrmark *et al.*, 2012) and reverse ITS4/ITS4arch (White *et al.*, 1990; Sterkenburg *et al.*, 2015) primers, both of

© 2022 The Authors
New Phytologist © 2022 New Phytologist Foundation

14698137, 2023, 6, Downloaded from https://nph.onlinelibrary.wiley.com/doi/10.1111/nph.18679 by Swedish University Of Agricultural Sciences, Wiley Online Library on [28/07/2023]. See the Terms and Conditions (https://onlinelibrary.wiley.com/terms-and-conditions) on Wiley Online Library for rules of use; OA articles are governed by the applicable Creative Commons License

which were extended by a linker base (T), sample-specific 8-base identification tags (which differed in at least three positions) and a terminal base (C) (Clemmensen *et al.*, 2016). Amplification was done with minimized numbers of PCR cycles to avoid length-based biases (reaction mix and cycle conditions are available in Table S1; Castaño *et al.*, 2020). Further details are available in Methods S1.

DNA sequence analyses

Sequences were quality-filtered and clustered using the SCATA pipeline (https://scata.mykopat.slu.se/, accessed on April 16, 2019). Sequences shorter than 200 bases were removed, and the remaining sequences were screened for primers (requiring 90% match) and sample tags (100% match). Sequences with an average amplicon quality score of < 20 or with a score of < 10 at any position were omitted. Unique genotypes in the total data set were removed to limit the influence of sequencing errors on the clustering outcome. After collapsing homopolymers to three bases, sequences were clustered into species-level clusters (hereafter 'species') using single-linkage clustering based on USEARCH (Edgar, 2010) pairwise comparisons with mismatch penalty of 1, gap open penalty of 0, gap extension penalty of 1, and a minimum similarity of 98.5% to the closest neighbor required to enter clusters. The entire UNITE database of fungal species hypotheses (Abarenkov *et al.*, 2010) and published reference data sets (Clemmensen *et al.*, 2014, 2021; Lindahl *et al.*, 2021) were included as reference data during clustering, providing taxonomical identification based on the same criteria as the clustering but without influencing the clustering outcome.

After the removal of clusters representing plants, 165 985 out of the total of 357 439 reads (1610 ± 65 reads per sample) remained. The 557 most abundant fungal species, each represented by at least 50 sequences and together representing *c.* 93% of total fungal reads, were evaluated further for taxonomical and functional classification. For this, the most abundant genotype from each species was compared against the UNITE and INSD databases using MASSBLASTER in PLUTOF (Abarenkov *et al.*, 2010), and the output carefully evaluated. A first full taxonomical profile of each species was also obtained using PROTAX (Somervuo *et al.*, 2016) implemented in PLUTOF, using a 50% probability of classification. Taxonomic identities at species level were assigned based on > 98.5% similarity with database references. Fungal species were further assigned to the following functional guilds based on information on their prevalent substrate and plant associations: root-associated basidiomycetes, root-associated ascomycetes, yeasts, saprotrophic basidiomycetes, saprotrophic ascomycetes, pathogens, molds, wood saprotrophs, lichens, and AM fungi.

Ectomycorrhizal (ECM) species were assigned to exploration types: contact, short, medium-smooth, medium-fringe, and long, according to Agerer (2001) and DEEMY (Agerer & Rambold, 2017).

Statistical analyses

Community data were analyzed with CANOCO v.5.0 (Biometris Plant Research International, Wageningen, the Netherlands), and univariate data were analyzed in R v.3.0.2 (R Core Team, 2021).

Our study was designed to minimize spatially confounding effects by targeting all vegetation types at each location. A Euclidean distance matrix based on Universal Transverse Mercator (UTM) coordinates of the plots was reduced into significant spatial principal coordinates of neighbor matrices (PCNM) vectors ($P < 0.05$). We then used variance partitioning to quantify variance attributed to spatial factors, vegetation types, and soil variables (C : N ratios, C stocks, N stocks, and $\delta^{15}N$). Conditional effects of these three variable groups (i.e. spatial, vegetation, and soil) were tested by redundancy analysis (RDA) with 999 Monte-Carlo permutations.

Initial analyses indicated that fungal communities and abundances of bacterial and archaeal functional genes were similar in the two humus horizons, with no vegetation type × horizon interactions found ($P > 0.05$). Hence, we based all further analyses of microbial communities on mass-weighed averages of the two humus layers, which also eliminated depth-wise pseudoreplication. To test whether soil fungal communities reflected vegetation types, we first used correspondence analysis (CA) of Hellinger-transformed fungal community data to obtain a graphical representation of community similarity among vegetation types. The effects of vegetation type on community composition were tested and visualized by canonical correspondence analysis (CCA) using Monte-Carlo permutation tests (999 permutations). Canonical correspondence analyses with forward selection of explanatory variables were also used to test whether soil factors indicative of N cycling mode (C : N and $\delta^{15}N$) and total N and C stocks per area were related to compositional and functional changes in fungal communities. To visualize patterns in microbial communities aggregated in functional groups, principal component analysis (PCA) was performed using the centered and standardized functional group abundances (*absolute abundances* of archaeal *amoA*, *nifH*, and *nrfA*; *relative abundances* of each fungal guild; and *ratios* of fungal and bacterial abundance) and the soil variables were correlated to the ordination axes.

We tested whether plot-level soil variables (i.e. total C and N stocks, C : N ratios, and $\delta^{15}N$) and gene copy numbers (bacteria, fungi, and the functional N cycling groups) differed significantly among the six vegetation types using linear mixed-effects models (in the NLME package), in which site ($n = 7$) was included as random factor and vegetation type as fixed factor. Models were checked for normality and homoscedasticity, and data were transformed when needed. Tukey's HSD (in the EMMEANS package to adjust for multiple testing) was used for *post hoc* tests ($P < 0.05$) of all pairwise comparisons.

Linear mixed-effects models were used to test associations between soil variables and abundance of microbial groups (bacterial 16S rRNA gene and fungal ITS abundance, bacterial and archaeal *amoA*, *nif*H and *nrf*A genes; relative abundance of fungal functional groups). These models were run separately with each individual microbial abundance specified as fixed factor, but additional models also included vegetation type as random factor to disentangle patterns within vegetation types.

© 2022 The Authors
New Phytologist © 2022 New Phytologist Foundation

14698137, 2023, 6, Downloaded from https://nph.onlinelibrary.wiley.com/doi/10.1111/nph.18679 by Swedish University Of Agricultural Sciences, Wiley Online Library on [28/07/2023]. See the Terms and Conditions (https://onlinelibrary.wiley.com/terms-and-conditions) on Wiley Online Library for rules of use; OA articles are governed by the applicable Creative Commons License

To understand how microbial communities interacted with long-term soil C and N dynamics, we compared depth profiles of C : N and $\delta^{15}N$ based on the two organic soil layers and the litter layer. Soil depth is a good representation of organic matter age in cold ecosystems with acidic soils and limited vertical mixing by burrowing fauna (Clemmensen *et al.*, 2013). The amount of organic matter above the sampling point ('depth-wise cumulative stocks') is a more reliable representation of soil depth than directly measured distances, which are confounded by variation in density and compaction during sampling. Therefore, we used depth-wise cumulative N stocks as a representation of depth (and organic matter age) to capture vertical variation in C : N ratio and ^{15}N-enrichment. Slope values of linear regressions of $\delta^{15}N$ values against depth-wise cumulative N stocks across the three depth layers in each plot were calculated as $s = r\,(\sigma X/\sigma Y)$, where s is the slope, σX is the SD of $\delta^{15}N$, σY is the SD of cumulative N stocks, and r is the correlation coefficient. We then used linear mixed-effects models to test relationships between the relative abundance of root-associated fungi, and (1) the soil C : N ratio (mass-weighed across all three layers per plot), and (2) the slope of $\delta^{15}N$ linearly regressed against the depth-wise cumulative N stock.

Results

Soil and microbial N cycling characteristics

C : N ratios in the organic topsoil (averaged across H1 and H2) were lowest in milking grounds (17 ± 1), intermediate in transitional samples, and highest in forests (26 ± 1) and heath (32 ± 2), whereas the $\delta^{15}N$ signatures showed the opposite pattern (Fig. 1; Table S2). Fungal : bacterial ratios were lowest in milking grounds and higher toward both heath and forest (Fig. 1; Table S2). The genetic potential for archaeal ammonia oxidation (i.e. archaeal *amoA* abundance) and respiratory ammonification (*nrfA* abundance) was highest in milking grounds, intermediate in transitions, and low or absent in both heath and forest (Fig. 1; Table S2). Bacterial *amoA* abundance was below detection limit. The genetic potential for soil-borne diazotrophic N_2 fixation (*nifH* abundance) by free-living bacteria was lowest in milking grounds and increased progressively toward the heath (Fig. 1; Table S2).

Fungal communities differed among vegetation types

Soil variables, vegetation types, and their shared variation explained 21.8% of total variation in fungal community composition, whereas spatial distance had a small (3.2%) but significant influence (Fig. S2). Fungal communities in milking grounds and heathlands were most divergent, while forest and areas undergoing colonization by either heath or trees had intermediary positions along the first axis of the CA ordination plot (Fig. 2a). CCA confirmed that fungal communities changed across vegetation types ($P < 0.001$, $R^2_{(adj)} = 10.7\%$; Fig. 2b). While several root-associated ascomycetes (e.g. *Hyaloscypha* and other *Helotiales* spp.) increased their dominance toward heath, root-associated basidiomycetes (e.g. *Pseudotomentella*, *Cortinarius*, and *Russula*) increased toward forest (Fig. 2b). There was a shift within the ECM fungal communities from the dominance of species with simple mycelia (contact, short, and medium-smooth exploration types) making up *c.* 98% of the ECM reads in plots recently colonized by trees, toward the dominance of cord-forming species (medium-fringe type), mainly *Cortinarius*, making up 20% of ECM reads under established trees and 83% of the ECM reads in mature forest (Fig. S3). Two AM clusters were found in milking grounds, but they accounted for < 1% of reads. A set of root-associated ascomycetes were present in milking grounds, including species of *Archaeorhizomyces*, *Oidiodendron*, and *Mollisia* as well as members of the order Helotiales (Fig. 2b). Molds (e.g. *Mortierella and*, *Umbelopsis*) and other saprotrophs, such as *Pseudeurotium* and yeasts (e.g. *Cryptococcus*), were also associated with milking grounds (Fig. 2b).

Mode of N cycling is linked to changes in the abundance of microbial guilds

The relative contribution of fungal guilds and abundances of genes involved in inorganic N cycling was aligned with soil factors along a gradient from lower C : N and higher pH, $\delta^{15}N$ and N stocks in milking grounds toward higher C : N and lower pH, $\delta^{15}N$ and N stocks in forest and heath (Fig. 3), with correlations underpinned by both among- and within-vegetation type variation (Fig. S4; Table S2). Carbon stocks were unrelated to this overall pattern. Heaths had the lowest average pH of 3.9 ± 0.2, and milking grounds had the highest average pH of 4.6 ± 0.1.

Abundance of *nrfA* and archaeal *amoA* genes and fungal saprotrophs increased with lower C : N ratios and higher N stocks typical of milking grounds (Fig. 3; Table S2). Litter C : N ratios were highest in heath (40 ± 3), lowest in forest (26 ± 3), and intermediate in milking grounds (33 ± 4), but C : N ratios decreased more steeply with soil depth in milking grounds than in heath and forest (Fig. 4a). By contrast, the $\delta^{15}N$ signature increased more steeply with soil depth in heath and forest than in milking grounds ($P < 0.01$; Fig. 4b). Soil C : N ratio was positively associated with fungal abundance (Fig. S4, Table S2), particularly root-associated fungi (Figs 3, 4c; Table S2). Similarly, the steeper increases in $\delta^{15}N$ with depth were positively related to the relative abundance of root-associated fungi ($F = 21.1$, $P < 0.001$, $R^2 = 37.4\%$, Fig. 4d).

Mycorrhizal fungi with contrasting decomposition capacities uncouple soil N and C storage across vegetation types

Soil N stocks differed more among vegetation types than soil C stocks. Soil N stocks reflected patterns in $\delta^{15}N$ with the highest levels in milking grounds and lower levels in both heath and forest (Fig. 1; Table S2). Soil C stocks were higher in the heath than in forests (Fig. 1; Table S2), but were not related to patterns in soil N stock, C : N or $\delta^{15}N$, fungal : bacterial ratio or inorganic N cycling potential in a consistent manner across vegetation types (Fig. 1). Along the milking ground-to-forest transitional

© 2022 The Authors
New Phytologist © 2022 New Phytologist Foundation

14698137, 2023, 6, Downloaded from https://nph.onlinelibrary.wiley.com/doi/10.1111/nph.18679 by Swedish University Of Agricultural Sciences, Wiley Online Library on [28/07/2023]. See the Terms and Conditions (https://onlinelibrary.wiley.com/terms-and-conditions) on Wiley Online Library for rules of use; OA articles are governed by the applicable Creative Commons License

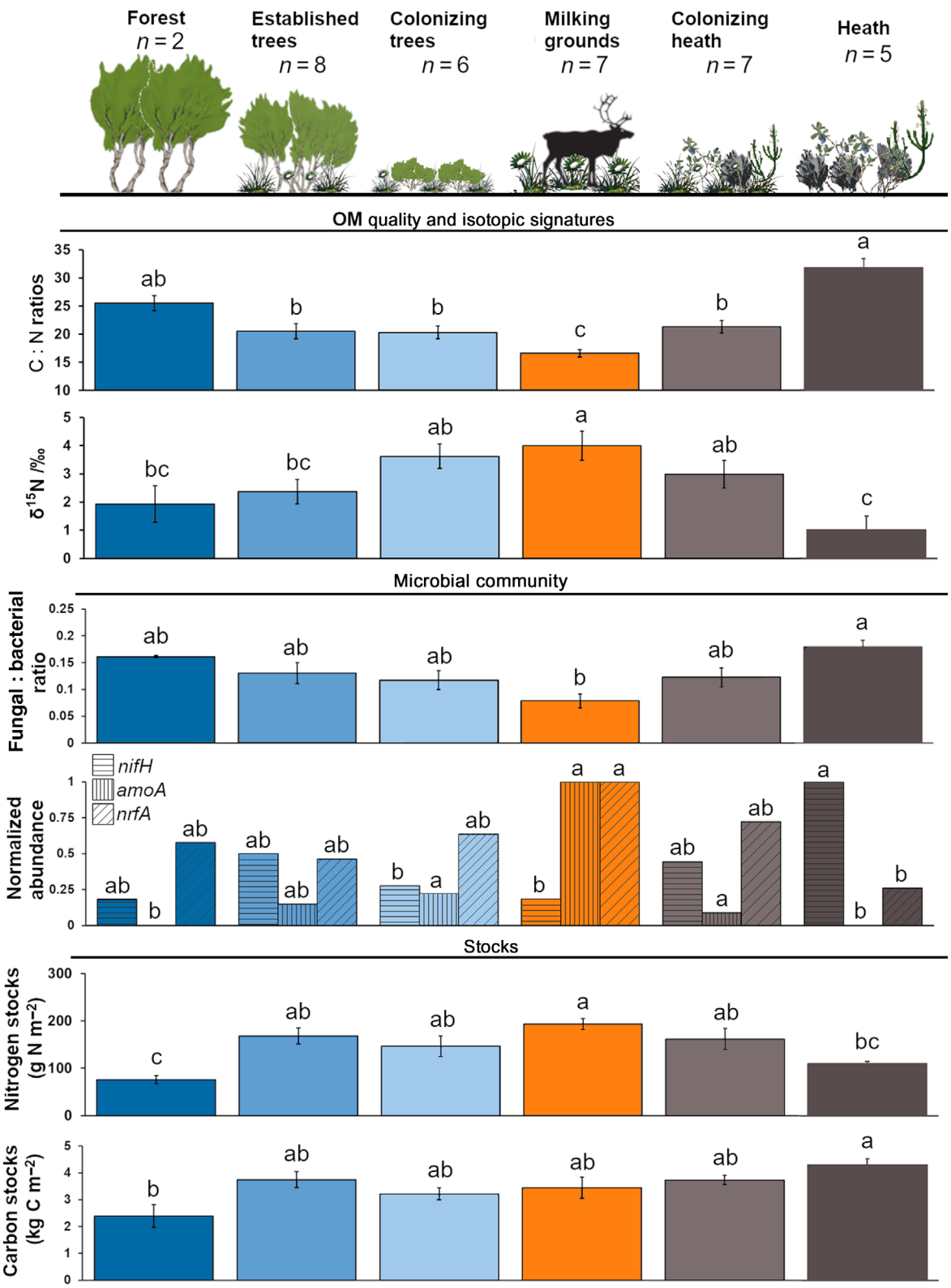

Fig. 1 Organic topsoil C : N ratios, δ^{15}N signatures, fungal : bacterial ratios, abundances of functional genes involved in inorganic N cycling (nifH, amoA, and nrfA; values rescaled from copies per g OM-1 to a range of [0,1] for each gene), and total N and C stocks in six vegetation types in Badjelánnda National Park. The total depth of the organic topsoil was 10–20 cm, and the superficial litter layer was only included for the C and N stocks. Error bars are SE of the means, and different letters indicate significant difference among vegetation types for each variable, as determined by Tukey's pairwise comparison test ($\alpha = 0.05$, $n = 2$–8).

© 2022 The Authors
New Phytologist © 2022 New Phytologist Foundation

14698137, 2023, 6, Downloaded from https://nph.onlinelibrary.wiley.com/doi/10.1111/nph.18679 by Swedish University Of Agricultural Sciences, Wiley Online Library on [28/07/2023]. See the Terms and Conditions (https://onlinelibrary.wiley.com/terms-and-conditions) on Wiley Online Library for rules of use; OA articles are governed by the applicable Creative Commons License

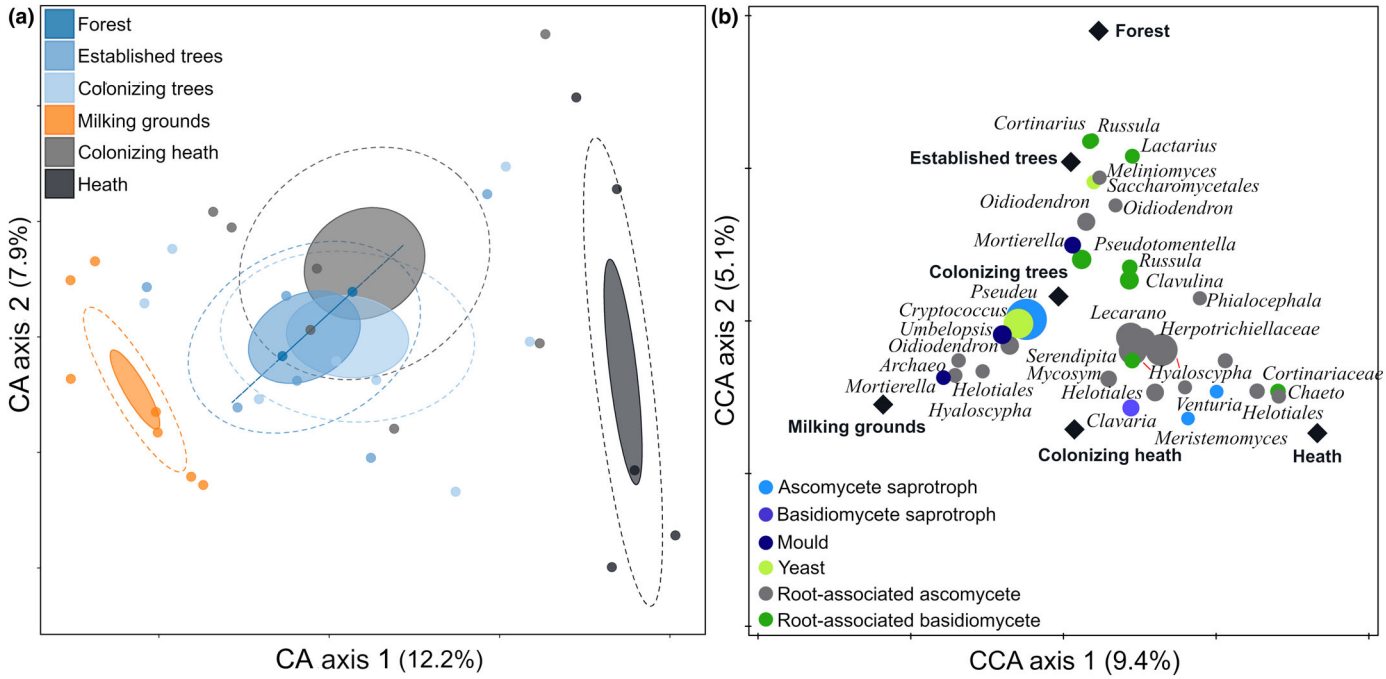

Fig. 2 Fungal community composition in the organic topsoil across vegetation types in Badjelánnda National Park, as analyzed by sequencing of ITS2 amplicons. (a) Sample plot of a correspondence analysis (CA) with vegetation types grouped by confidence intervals (inner circles, 5%, and dotted outer circles, 75%), and (b) species plot of a canonical correspondence analysis (CCA) with axes constrained by vegetation types (black diamonds; $P < 0.001$) showing the 32 most abundant fungal species and their taxonomic and functional classification (colored circles). Archaeo, *Archaeorhizomyces*; Chaeto, *Chaetomium*; Mycosym, *Mycosymbioses*; Pseudeu, *Pseudeurotium*; Lecanoro, *Lecanoromycetes*.

gradient, both C and N stocks declined, whereas along the milking ground-to-heath gradient N stocks decreased while C stocks remained high. Thus, milking grounds, forests, and heaths stabilize at different soil C : N ratios as they accumulate soil C and N stocks at different rates (Figs 1, S5).

Fungal community composition was significantly correlated with both N (Pseudo-$F = 1.6$, $P_{(adj)} = 0.004$, Adj. expl = 4.8%) and C stocks (Pseudo-$F = 2.2$, $P_{(adj)} = 0.002$, Adj. expl = 6.2%). A large group of root-associated ascomycetes and some root-associated basidiomycetes, prevalent in heath, correlated negatively with N stocks, but positively with C stocks (Fig. S6). By contrast, several root-associated basidiomycetes, prevalent in forest, such as ECM species within *Cortinarius*, *Russula*, *Piloderma*, and *Lactarius*, correlated negatively with both N and C stocks (Fig. S6). Molds, such as species of *Mortierella*, and some root-associated ascomycetes within *Archaeorhizomyces* and *Oidiodendron* associated with the high N and C stocks of some milking grounds and transitional plots (Fig. S6).

Discussion

Our study of a stable mosaic of grasslands (historical reindeer milking grounds) and close-by forest and heath vegetation allowed us to test hypotheses derived from larger-scale vegetation patterns (Read, 1991; Steidinger *et al.*, 2019) of how distinct plant–microbial interactions affect N and C cycling and stocks with limited confounding effects of climatic variation or other large-scale drivers. In addition, the studied indicators of plant–microbial feedbacks allowed us to evaluate stabilization mechanisms operating along, and potentially maintaining, abrupt changes among the vegetation types. The inclusion of areas more recently colonized by trees or heath vegetation corroborated the proposed causal relationships between microbial community composition and soil processes across the vegetation mosaic.

Overall, our data support the idea that contrasting plant–microbial feedback mechanisms, involving different modes of N cycling, act to stabilize the three vegetation types, in line with the predictions of our first hypothesis. However, AM fungi were less abundant in the grasslands than expected. Our second hypothesis predicted that C and N stocks would show disparate patterns across these vegetation types, along with the different feedbacks. This hypothesis was also supported, as C stocks differed much less than N stocks among vegetation types. However, grasslands had larger C stocks than expected. Below follows a proposal (Fig. 5) of how the vegetation types are maintained by contrasting positive feedbacks and how these may have resulted in the observed C and N stock patterns across the vegetation mosaic.

Historical milking grounds are the result of previous intensive reindeer husbandry practices, which incurred disturbance and accumulation of nutrients during past centuries. The absence of AM fungi in milking grounds was unexpected, as the vegetation was dominated by grasses and forbs typically associated with AM fungi (Egelkraut *et al.*, 2018a,b). Instead, we detected particular species of dark septate root endophytes and other putative root-associated ascomycetes, which are common in Antarctic and Arctic ecosystems (Newsham *et al.*, 2009). These fungi are generally well protected against harsh conditions by thick and melanized cell walls (Fernandez & Koide, 2013), and some have been found

© 2022 The Authors
New Phytologist © 2022 New Phytologist Foundation

14698137, 2023, 6, Downloaded from https://nph.onlinelibrary.wiley.com/doi/10.1111/nph.18679 by Swedish University Of Agricultural Sciences, Wiley Online Library on [28/07/2023]. See the Terms and Conditions (https://onlinelibrary.wiley.com/terms-and-conditions) on Wiley Online Library for rules of use; OA articles are governed by the applicable Creative Commons License

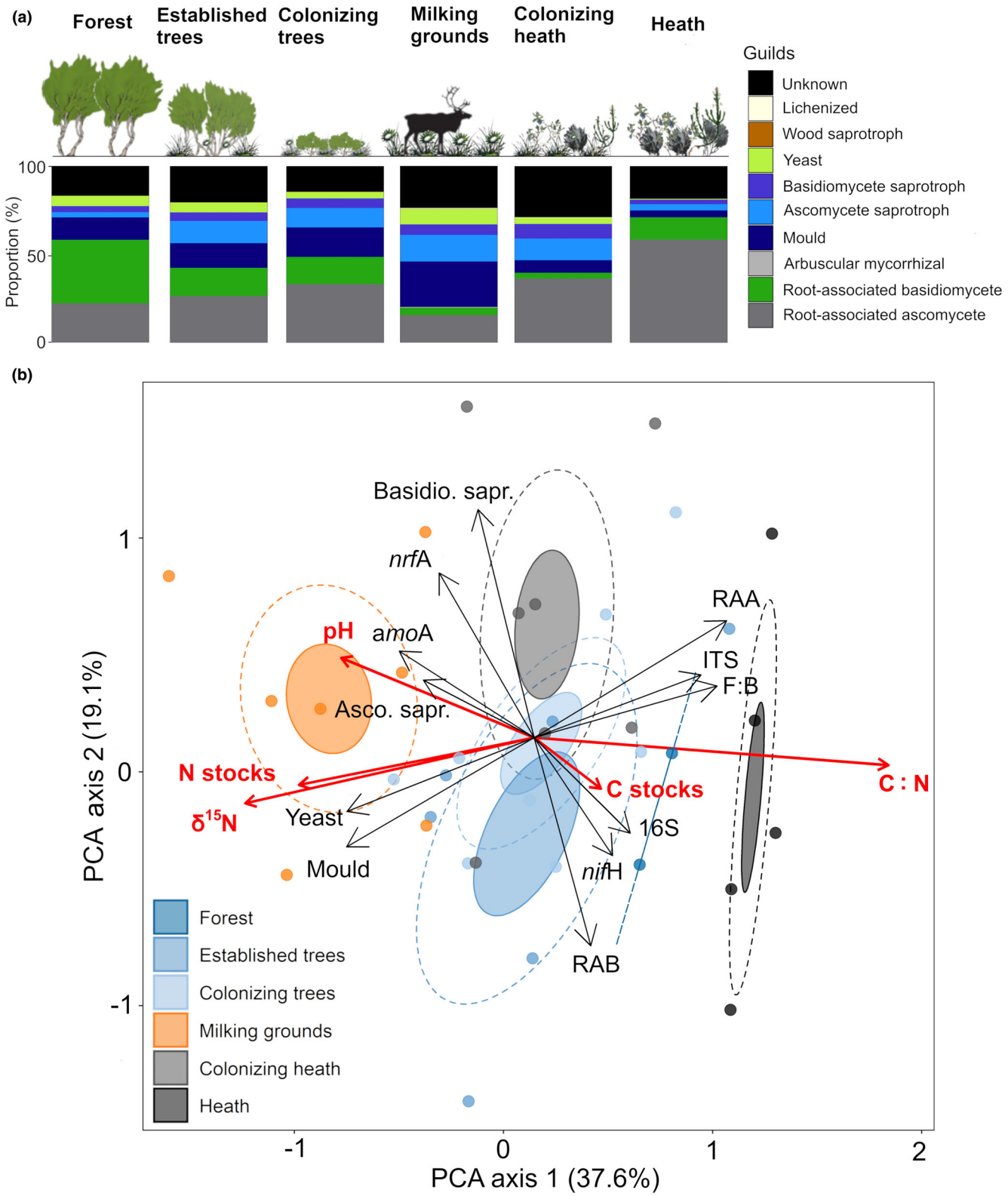

Fig. 3 Functional characteristics of fungal and prokaryotic communities in the organic topsoil of six vegetation types in Badjelánnda National Park, based on sequencing of ITS2 amplicons and quantification of functional genes, respectively. (a) Relative abundances of fungal functional groups in the organic topsoil in each vegetation type. (b) Principal components analysis (PCA) of fungal guilds and bacterial and archaeal functional genes involved in inorganic nitrogen cycling (black arrows) and relationships with soil variables (red arrows). The soil parameters were passively fitted to the ordination axes, and length of arrows reflects the strength of association with the PCA axes. Vegetation types are grouped by confidence intervals (inner circles, 5%, and dotted outer circles, 75%). Microbial components were centered and standardized. Asco. sapr., Ascomycete saprotrophs; Basidio. sapr., Basidiomycetes saprotrophs; F : B, fungal : bacterial ratio; RAA, root-associated ascomycetes; RAB, root-associated basidiomycetes.

© 2022 The Authors
New Phytologist © 2022 New Phytologist Foundation

14698137, 2023, 6, Downloaded from https://nph.onlinelibrary.wiley.com/doi/10.1111/nph.18679 by Swedish University Of Agricultural Sciences, Wiley Online Library on [28/07/2023]. See the Terms and Conditions (https://onlinelibrary.wiley.com/terms-and-conditions) on Wiley Online Library for rules of use; OA articles are governed by the applicable Creative Commons License

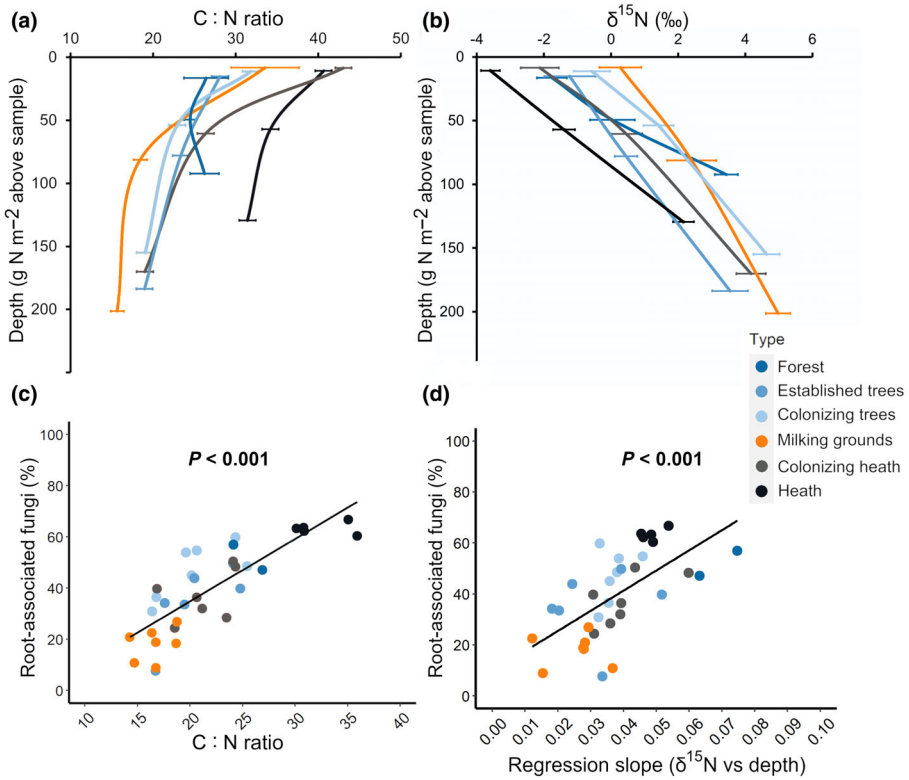

Fig. 4 Depth profiles of (a) C : N ratios and (b) $\delta^{15}N$ (‰) in the organic topsoil of six vegetation types. Values for three depth layers (the superficial litter layer and the two deeper humus layers) are plotted against depth-wise cumulative N stocks. Relative abundances of root-associated fungi (summed Ascomycota and Basidiomycota) plotted against (c) the organic topsoil C : N ratios (mass-weighed over the three organic horizons per plot), and (d) the regression slopes of $\delta^{15}N$ against depth-wise cumulative N stocks (as in b, but with slopes obtained from linear regressions per sampling plot). Total depth of the organic topsoil was 10–20 cm. The lines and *P*-values in (c) and (d) are linear regressions across all 35 plots. Error bars are SE of the means (n = 2–7 per vegetation type).

to be favored by high soil N availability (Kytöviita & Olofsson, 2021) or may promote plant performance by mineralizing N in the vicinity of the roots (Newsham *et al.*, 2009; Newsham, 2011). Even a century after active use ceased, the grasslands had the largest proportion of free-living saprotrophic fungi, with molds, yeasts, and ascomycete saprotrophs being particularly important. These groups typically mediate fast decomposition of relatively high-quality organic matter, such as recent plant litter and dead mycelium. Together with the low fungal-to-bacteria ratios (based on gene copy ratios) and high genetic potential for ammonia oxidation and respiratory ammonification, this suggests fast decomposition, mineralization, and inorganic N cycling (Phillips *et al.*, 2013; Lin *et al.*, 2017). We found no evidence for currently enhanced N inputs through diazotrophic N fixation by free-living bacteria, as the *nifH* abundance was low in the grasslands. Instead, the higher genetic potentials for respiratory ammonification in grasslands suggest elevated nitrification and that recycling of nitrate to ammonium can be an important mechanism that minimizes N losses and retains large N stocks in this system (Putz *et al.*, 2018). We speculate that this inorganic N cycling and retention by DNRA bacteria underlie the previously suggested positive plant–soil feedbacks in milking grounds (Egelkraut *et al.*, 2018b), which would favor the persistence of fast-growing, high-litter-quality plants. The $\delta^{15}N$ signatures were also particularly high in grasslands (Fig. 1), probably due to ^{15}N-enriched inputs, and potentially also losses of ^{15}N-depleted N during the reindeer grazing legacy (Högberg *et al.*, 1996). Based on our results, we propose that, unless inorganic pools are depleted, these grassland patches may be resistant to colonization by less competitive birch seedlings and ericaceous shrubs (Fig. 5).

The increasing organic topsoil C : N ratios when transitioning from grasslands to either forest or heath were associated with decreasing genetic potentials for inorganic N cycling and increasing relative abundance of root-associated fungi. Together these patterns suggest that root-associated fungi promoted shifts from inorganic to organic N cycling along both gradients (Clemmensen *et al.*, 2013; Phillips *et al.*, 2013). The summed relative abundance of all ECM fungi increased toward forest, but there was also a shift within ECM communities. Several of the ECM fungi that dominated in forest soils, such as species within *Russula* and *Cortinarius*, correlated negatively with both C and N stocks, and particularly *Cortinarius* species have previously been suggested to be efficient decomposers that mine N from older organic matter (Bödeker *et al.*, 2014; Lindahl & Tunlid, 2015). Such potential N mining activity would be consistent with the steeper depth gradient in $\delta^{15}N$ and higher C : N ratios in deeper organic layers observed in the forest, as both of these patterns can result from ECM fungal N mobilization and transfer of ^{15}N-depleted N to plant hosts (Hobbie & Högberg, 2012; Clemmensen *et al.*, 2013). In contrast to forests, under higher inorganic N availability in, or close to, former milking grounds, the relative abundance of ECM fungi was lower, and potential N mining ECM had lower relative abundance (established trees) or were absent (colonizing trees). This suggests that while trees colonizing former grasslands from the edges may mainly exploit easily available N pools, ECM decomposers increase in abundance only

© 2022 The Authors
New Phytologist © 2022 New Phytologist Foundation

14698137, 2023, 6, Downloaded from https://nph.onlinelibrary.wiley.com/doi/10.1111/nph.18679 by Swedish University Of Agricultural Sciences, Wiley Online Library on [28/07/2023]. See the Terms and Conditions (https://onlinelibrary.wiley.com/terms-and-conditions) on Wiley Online Library for rules of use; OA articles are governed by the applicable Creative Commons License

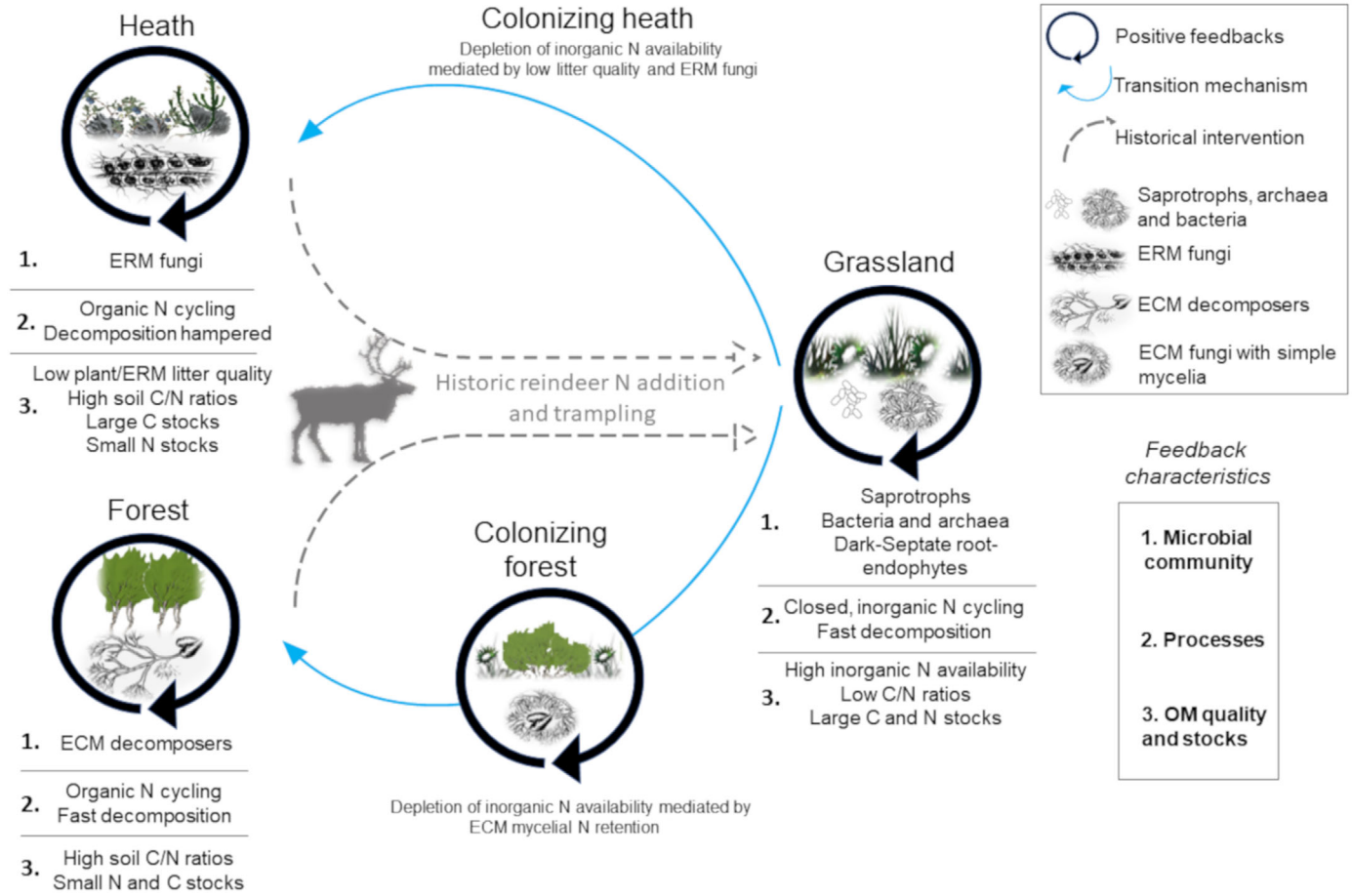

Fig. 5 Scheme summarizing the proposed stabilizing plant–microbial feedbacks and their indicators (dominant microbial community members, soil processes, and organic matter quality and stocks) in historical milking grounds (grasslands) and surrounding heath and forest vegetation in Badjelánnda National Park, based on the results of this study. Contrasting plant–microbial feedbacks (shown in black arrows) act as self-reinforcing drivers of the three vegetation trajectories by excluding competing biota. Initially, in transitional areas (i.e. forest and heath colonization), such plant–microbial feedbacks are weak, but progressively self-reinforced by coordinated changes in multiple soil and vegetation factors. The proposed stabilizing plant–microbial feedbacks can cause abrupt changes in vegetation even at local geographical scales (e.g. < 100 m) and under similar environmental conditions. Which plant–microbial feedbacks dominate will determine organic matter quality of both plants and microbes and the decomposition capacity of the microbial communities, both of which will have cascading effects on nutrient cycling and on soil C and N stocks. In forests, limiting N availability promotes ECM decomposers that can oxidize organic matter, decreasing soil N and C stocks. In heath, plant–fungal litter interactions stabilize organic matter. We postulate that these contrasting plant–microbial feedbacks drive the long-term stability of the three contrasting vegetation types.

under N limitation further away from the grasslands. Based on our results and previous work, we speculate that ECM decomposers restrict the accumulation of soil N and C (Clemmensen *et al.*, 2021; Lindahl *et al.*, 2021), thus promoting a positive plant–soil feedback loop that allows trees to access and monopolize an otherwise inaccessible N pool in the forest (Fig. 5). If trees colonize ancient grasslands, a long-term consequence of this feedback may be a loss of the soil C and N stocks accumulated during the grazing legacy, as subarctic birch forest typically hold only 1–2 kg C m^{-2} and 10–15 g N m^{-2} in aboveground biomass (Hartley *et al.*, 2012), compared with the > 100 g N m^{-2} difference in soil pools between milking grounds and forests. However, our current sampling design did not allow us to assess whether invading trees could elicit net ecosystem losses of C and N, for which longer time series of tree colonization of former grasslands would be needed. The large soil C and N stocks under colonizing and established trees suggest a rather stable ecosystem state with maintained belowground pools, in spite of increasing tree biomass, potentially maintained by continued inorganic N cycling and retention. Unfortunately, our study system only included two mature control forests, which constrained our statistical power and potentially the generality of our results. However, all soil and community characteristics of our control forests were similar to those in previous studies of similar sites (Hartley *et al.*, 2012; Parker *et al.*, 2015, 2021; Clemmensen *et al.*, 2021; Ylänne *et al.*, 2021).

The heath had the highest C : N ratio of the organic topsoil, which paralleled high litter layer C : N ratios. Nevertheless, the dominance of root-associated fungi and their positive association with C : N ratios suggests that root-mediated processes are important in regulating organic soil C and N dynamics and total stocks. Relative abundance of root-associated ascomycetes and ERM fungi, particularly *Hyaloscypha* spp., also increased progressively from milking grounds toward heath. Soil C stocks however

© 2022 The Authors
New Phytologist © 2022 New Phytologist Foundation

14698137, 2023, 6, Downloaded from https://nph.onlinelibrary.wiley.com/doi/10.1111/nph.18679 by Swedish University Of Agricultural Sciences, Wiley Online Library on [28/07/2023]. See the Terms and Conditions (https://onlinelibrary.wiley.com/terms-and-conditions) on Wiley Online Library for rules of use; OA articles are governed by the applicable Creative Commons License

14698137, 2023, 6, Downloaded from https://nph.onlinelibrary.wiley.com/doi/10.1111/nph.18679 by Swedish University Of Agricultural Sciences, Wiley Online Library on [28/07/2023]. See the Terms and Conditions (https://onlinelibrary.wiley.com/terms-and-conditions) on Wiley Online Library for rules of use; OA articles are governed by the applicable Creative Commons License

did not differ between heath and milking grounds (Stark *et al.*, 2019), but C stocks were less variable than N stocks and consistently high in heaths. The maintained C stocks in heath may seem counterintuitive, since ERM fungi have the capacity to access a wide range of organic substrates (Read & Perez-Moreno, 2003; Martino *et al.*, 2018). However, ERM fungi do not possess oxidative mechanisms to attack complex, phenolic macromolecules (e.g. lignin), typical for white-rot (extracellular peroxidases) or brown-rot (Fenton chemistry) Basidiomycota. Moreover, ERM necromass can be stabilized by interacting with plant tannins (Adamczyk *et al.*, 2019) and often has relatively high C : N ratios, lipid, and melanin concentrations, which makes it resistant to decomposition (Fernandez & Kennedy, 2018). Additionally, *nifH* genes were most abundant in heath, indicating that some of the N needed by the plants may be supplied through fixed N rather than through decomposition. We propose that low-quality plant and fungal litter and fungal communities without prominent decomposer capacities impair decomposition and N mineralization (Wardle *et al.*, 2003), leading to strong positive plant–soil feedbacks that preserves the stress-adapted plant and fungal communities in the heath and precludes the establishment of faster-growing plant species (Read, 1991; Fig. 5).

In conclusion, more than a century after abandonment, the historical milking grounds still show multiple indications of prominent inorganic N cycling, likely maintaining dominance by grassland vegetation through a positive plant–soil–microbial feedback loop (Fig. 5). Only along the grassland edges, where trees or dwarf shrubs and their root-associated fungi had colonized within the last 50 yr, we observed decreasing inorganic N cycling potential and increasing soil C : N ratios. This suggests that unless inorganic pools are depleted, these grassland patches may be resistant to colonization by less competitive trees or shrubs. Heath and forest vegetation also showed indications of positive plant–soil–microbial feedbacks, albeit based on different mechanisms. While trees seemed to support organic matter decomposition and organic N mobilization via association with presumed efficient ECM decomposers, heath vegetation may hamper decomposition and N cycling by associating with stress-resistant root-associated ascomycetes. Meta-transcriptomics analyses would be a valuable approach to contrast N mining and decomposition activities across different soil communities, although sampling of rapidly degrading mRNA remains a challenge in remote areas like this. We propose that the contrasting plant–soil–microbial feedback mechanisms underlie the coordinated and abrupt patterns in multiple biotic and soil factors and stabilize the vegetation mosaic (Suz *et al.*, 2021) even in the absence of strong climatic drivers (cf. Steidinger *et al.*, 2019). We further propose that the disparate patterns in topsoil N and C stocks across the vegetation mosaic are tightly linked to contrasting ecologies of the root-associated fungal communities and the N cycling potential of the bacterial and archaeal communities (Fig. 5).

Acknowledgements

This work was funded by grants from Swedish University of Agricultural Sciences. The authors would like to acknowledge support of the Uppsala Genome Center and UPPMAX for providing assistance in massive parallel sequencing and computational infrastructure. Work performed at Uppsala Genome Center has been funded by VR (Vetenskapsrådet) and Science for Life Laboratory, Sweden. Jaanis Juhanson is acknowledged for advice on quantitative PCR. We acknowledge the valuable contributions of four anonymous reviewers.

Competing interests

None declared.

Author contributions

JO, DE, KEC and CC designed the experiment. The sequencing work and bioinformatic analyses were performed by CC with the support of KEC. The qPCR work was performed by CC with the support of SH. Data analysis was performed by CC with the support of KEC and BDL. The manuscript was written by CC with inputs from all authors.

ORCID

Carles Castaño https://orcid.org/0000-0002-2403-7006
Karina Engelbrecht Clemmensen https://orcid.org/0000-0002-9627-6428
Dagmar Egelkraut https://orcid.org/0000-0002-2644-2144
Sara Hallin https://orcid.org/0000-0002-9069-9024
Björn D. Lindahl https://orcid.org/0000-0002-3384-4547
Johan Olofsson https://orcid.org/0000-0002-6943-1218

Data availability

Sequence data are archived at NCBI's Sequence Read Archive under accession no. PRJNA750897. Experimental design, community data, and associated data of this study can be found in Mendeley Data/Dryad, doi: 10.17632/ptj93pcpfk.1.

References

Abarenkov K, Henrik Nilsson R, Larsson K-H, Alexander IJ, Eberhardt U, Erland S, Høiland K, Kjøller R, Larsson E, Pennanen T *et al.* 2010. The UNITE database for molecular identification of fungi – recent updates and future perspectives. *New Phytologist* **186**: 281–285.

Adamczyk B, Ahvenainen A, Sietiö OM, Kanerva S, Kieloaho AJ, Smolander A, Kitunen V, Saranpää P, Laakso T, Straková P *et al.* 2016. The contribution of ericoid plants to soil nitrogen chemistry and organic matter decomposition in boreal forest soil. *Soil Biology and Biochemistry* **103**: 394–404.

Adamczyk B, Sietiö O-M, Biasi C, Heinonsalo J. 2019. Interaction between tannins and fungal necromass stabilizes fungal residues in boreal forest soils. *New Phytologist* **223**: 16–21.

Agerer R. 2001. Exploration types of ectomycorrhizae. A proposal to classify ectomycorrhizal mycelial systems according to their patterns of differentiation and putative ecological importance. *Mycorrhiza* **11**: 107–114.

Agerer R, Rambold G. 2017. *Deemy – an information system for characterization and determination of ectomycorrhizae.* München, Germany: www.deemy.de.

Averill C, Turner BL, Finzi AC. 2014. Mycorrhiza-mediated competition between plants and decomposers drives soil carbon storage. *Nature* **505**: 543–545.

Bell T, Freckleton RP, Lewis OT. 2006. Plant pathogens drive density-dependent seedling mortality in a tropical tree. *Ecology Letters* **9**: 569–574.

Bennett JA, Klironomos J. 2019. Mechanisms of plant–soil feedback: interactions among biotic and abiotic drivers. *New Phytologist* **222**: 91–96.

Bennett JA, Maherali H, Reinhart KO, Lekberg Y, Hart MM, Klironomos J. 2017. Plant–soil feedbacks and mycorrhizal type influence temperate forest population dynamics. *Science* **355**: 181–184.

Bödeker ITM, Clemmensen KE, de Boer W, Martin F, Olson Å, Lindahl BD. 2014. Ectomycorrhizal *Cortinarius* species participate in enzymatic oxidation of humus in northern forest ecosystems. *New Phytologist* **203**: 245–256.

Castaño C, Berlin A, Durling MB, Ihrmark K, Lindahl BD, Stenlid J, Clemmensen KE, Olson Å. 2020. Optimized metabarcoding with Pacific biosciences enables semi-quantitative analysis of fungal communities. *New Phytologist* **228**: 1149–1158.

Clemmensen KE, Bahr A, Ovaskainen O, Dahlberg A, Ekblad A, Wallander H, Stenlid J, Finlay RD, Wardle DA, Lindahl BD. 2013. Roots and associated fungi drive long-term carbon sequestration in boreal forest. *Science* **339**: 1615–1618.

Clemmensen KE, Durling MB, Michelsen A, Hallin S, Finlay RD, Lindahl BD. 2021. A tipping-point in carbon storage when forest expands into tundra is related to mycorrhizal recycling of nitrogen. *Ecology Letters* **24**: 1193–1204.

Clemmensen KE, Finlay RD, Dahlberg A, Stenlid J, Wardle DA, Lindahl BD. 2014. Carbon sequestration is related to mycorrhizal fungal community shifts during long-term succession in boreal forests. *New Phytologist* **205**: 1525–1536.

Clemmensen KE, Ihrmark K, Durling MB, Lindahl BD. 2016. Sample preparation for fungal community analysis by high-throughput sequencing of barcode amplicons. *Methods in Molecular Biology* **1399**: 61–88.

Cornelissen J, Aerts R, Cerabolini B, Werger M, Van der Heijden M. 2001. Carbon cycling traits of plant species are linked with mycorrhizal strategy. *Oecologia* **129**: 611–619.

Cornwell WK, Cornelissen JHC, Amatangelo K, Dorrepaal E, Eviner VT, Godoy O, Hobbie SE, Hoorens B, Kurokawa H, Pérez-Harguindeguy N *et al.* 2008. Plant species traits are the predominant control on litter decomposition rates within biomes worldwide. *Ecology Letters* **11**: 1065–1071.

Edgar RC. 2010. Search and clustering orders of magnitude faster than BLAST. *Bioinformatics* **26**: 2460–2461.

Egelkraut D, Aronsson K-Å, Allard A, Åkerholm M, Stark S, Olofsson J. 2018a. Multiple feedbacks contribute to a centennial legacy of reindeer on tundra vegetation. *Ecosystems* **21**: 1545–1563.

Egelkraut D, Kardol P, De Long JR, Olofsson J. 2018b. The role of plant–soil feedbacks in stabilizing a reindeer-induced vegetation shift in subarctic tundra. *Functional Ecology* **32**: 1959–1971.

Fanin N, Clemmensen KE, Lindahl BD, Farrell M, Nilsson M-C, Gundale MJ, Kardol P, Wardle DA. 2022. Ericoid shrubs shape fungal communities and suppress organic matter decomposition in boreal forests. *New Phytologist* **236**: 684–697.

Fernandez CW, Kennedy PG. 2018. Melanization of mycorrhizal fungal necromass structures microbial decomposer communities. *Journal of Ecology* **106**: 468–479.

Fernandez CW, Koide RT. 2013. The function of melanin in the ectomycorrhizal fungus Cenococcum geophilum under water stress. *Fungal Ecology* **6**: 479–486.

Hartley IP, Garnett MH, Sommerkorn M, Hopkins DW, Fletcher BJ, Sloan VL, Phoenix GK, Wookey PA. 2012. A potential loss of carbon associated with greater plant growth in the European Arctic. *Nature Climate Change* **2**: 875–879.

Hewitt RE, DeVan MR, Lagutina IV, Genet H, McGuire AD, Taylor DL, Mack MC. 2015. Mycobiont contribution to tundra plant acquisition of permafrost-derived nitrogen. *New Phytologist* **226**: 126–141.

Hobbie EA, Högberg P. 2012. Nitrogen isotopes link mycorrhizal fungi and plants to nitrogen dynamics. *New Phytologist* **196**: 367–382.

Hobbie JE, Hobbie EA. 2006. ^{15}N in symbiotic fungi and plants estimates nitrogen and carbon flux rates in arctic tundra. *Ecology* **87**: 816–822.

Högberg P, Hogbom L, Schinkel H, Hogberg M, Johannisson C, Wallmark H. 1996. ^{15}N abundance of surface soils, roots and mycorrhizas in profiles of European forest soils. *Oecologia* **108**: 207–214.

Ihrmark K, Bödeker ITM, Cruz-Martinez K, Friberg H, Kubartova A, Schenck J, Strid Y, Stenlid J, Brandström-Durling M, Clemmensen KE *et al.* 2012. New primers to amplify the fungal ITS2 region – evaluation by 454-sequencing of artificial and natural communities. *FEMS Microbiology Ecology* **82**: 666–677.

Keller AB, Phillips RP. 2019. Leaf litter decay rates differ between mycorrhizal groups in temperate, but not tropical, forests. *New Phytologist* **222**: 556–564.

Kohler A, Kuo A, Nagy LG, Morin E, Barry KW, Buscot F, Canbäck B, Choi C, Cichocki N, Clum A *et al.* 2015. Convergent losses of decay mechanisms and rapid turnover of symbiosis genes in mycorrhizal mutualists. *Nature Genetics* **47**: 410–415.

Kytöviita MM, Olofsson J. 2021. Idiosyncratic responses to simulated herbivory by root fungal symbionts in a subarctic meadow. *Arctic, Antarctic and Alpine Research* **53**: 80–92.

Lance AC, Carrino-Kyker SR, Burke DJ, Burns JH. 2020. Individual plant–soil feedback effects influence tree growth and rhizosphere fungal communities in a temperate forest restoration experiment. *Frontiers in Ecology and Evolution* **7**: 1–12.

Lin G, McCormack ML, Ma C, Guo D. 2017. Similar below-ground carbon cycling dynamics but contrasting modes of nitrogen cycling between arbuscular mycorrhizal and ectomycorrhizal forests. *New Phytologist* **213**: 1440–1451.

Lindahl BD, Kyaschenko J, Varenius K, Clemmensen KE, Dahlberg A, Karltun E, Stendahl J. 2021. A group of ectomycorrhizal fungi restricts organic matter accumulation in boreal forest. *Ecology Letters* **24**: 1341–1351.

Lindahl BD, Tunlid A. 2015. Ectomycorrhizal fungi – potential organic matter decomposers, yet not saprotrophs. *New Phytologist* **205**: 1443–1447.

López-Gutiérrez JC, Henry S, Hallet S, Martin-Laurent F, Catroux G, Philippot L. 2004. Quantification of a novel group of nitrate-reducing bacteria in the environment by real-time PCR. *Journal of Microbiological Methods* **57**: 399–407.

Mangan SA, Schnitzer SA, Herre EA, Mack KML, Valencia MC, Sanchez EI, Bever JD. 2010. Negative plant–soil feedback predicts tree-species relative abundance in a tropical forest. *Nature* **466**: 752–755.

Martino E, Morin E, Grelet G-A, Kuo A, Kohler A, Daghino S, Barry KW, Cichocki N, Clum A, Dockter RB *et al.* 2018. Comparative genomics and transcriptomics depict ericoid mycorrhizal fungi as versatile saprotrophs and plant mutualists. *New Phytologist* **217**: 1213–1229.

Marusina AI, Boulygina ES, Kuznetsov BB, Tourova TP, Kravchenko IK, Gal'chenko VF. 2001. A system of oligonucleotide primers for the amplification of nifH genes of different taxonomic groups of prokaryotes. *Microbiology* **70**: 73–78.

Newsham KK. 2011. A meta-analysis of plant responses to dark septate root endophytes. *New Phytologist* **190**: 783–793.

Newsham KK, Upson R, Read DJ. 2009. Mycorrhizas and dark septate root endophytes in polar regions. *Fungal Ecology* **2**: 10–20.

Northup RR, Yu Z, Dahlgren RA, Vogt KA. 1995. Polyphenol control of nitrogen release from pine litter. *Nature* **377**: 227–229.

Op De Beeck M, Troein C, Peterson C, Persson P, Tunlid A. 2018. Fenton reaction facilitates organic nitrogen acquisition by an ectomycorrhizal fungus. *New Phytologist* **218**: 335–343.

Parker TC, Subke JA, Wookey PA. 2015. Rapid carbon turnover beneath shrub and tree vegetation is associated with low soil carbon stocks at a subarctic treeline. *Global Change Biology* **21**: 2070–2081.

Parker TC, Thurston AM, Raundrup K, Subke JA, Wookey PA, Hartley AP. 2021. Shrub expansion in the Arctic may induce large-scale carbon losses due to changes in plant–soil interactions. *Plant and Soil* **463**: 643–651.

Phillips RP, Brzostek E, Midgley MG. 2013. The mycorrhizal-associated nutrient economy: a new framework for predicting carbon–nutrient couplings in temperate forests. *New Phytologist* **199**: 41–51.

Putz M, Schleusner P, Rütting T, Hallin S. 2018. Relative abundance of denitrifying and DNRA bacteria and their activity determine nitrogen retention or loss in agricultural soil. *Soil Biology and Biochemistry* **123**: 97–104.

R Core Team. 2021. *R: a language and environment for statistical computing.* Vienna, Austria: R Foundation for Statistical Computing. [WWW document] URL https://www.R-project.org/ [accessed 11 January 2021].

Read DJ. 1991. Mycorrhizas in ecosystems. *Experientia* **47**: 376–391.

© 2022 The Authors
New Phytologist © 2022 New Phytologist Foundation

14698137, 2023, 6, Downloaded from https://nph.onlinelibrary.wiley.com/doi/10.1111/nph.18679 by Swedish University Of Agricultural Sciences, Wiley Online Library on [28/07/2023]. See the Terms and Conditions (https://onlinelibrary.wiley.com/terms-and-conditions) on Wiley Online Library for rules of use; OA articles are governed by the applicable Creative Commons License

Read DJ, Perez-Moreno J. 2003. Mycorrhizas and nutrient cycling in ecosystems – a journey towards relevance? *New Phytologist* **157**: 475–492.

Rineau F, Roth D, Shah F, Smits M, Johansson T, Canbäck B, Olsen PB, Persson P, Grell MN, Lindquist E *et al.* 2012. The ectomycorrhizal fungus *Paxillus involutus* converts organic matter in plant litter using a trimmed brown-rot mechanism involving Fenton chemistry. *Environmental Microbiology* **14**: 1477–1487.

Robinson D. 2001. δ^{15}N as an integrator of the nitrogen cycle. *Trends in Ecology and Evolution* **16**: 153–162.

Rotthauwe JH, Witzel KP, Liesack W. 1997. The ammonia monooxygenase structural gene amoa as a functional marker: molecular fine-scale analysis of natural ammonia-oxidizing populations. *Applied and Environmental Microbiology* **63**: 4704–4712.

Rousk J, Bengtson P. 2014. Microbial regulation of global biogeochemical cycles. *Frontiers in Microbiology* **5**: 103.

Smith SE, Read DJ. 2008. *Mycorrhizal symbiosis, 3rd edn.* London, UK: Academic Press.

Somervuo P, Koskela S, Pennanen J, Henrik Nilsson R, Ovaskainen O. 2016. Unbiased probabilistic taxonomic classification for DNA barcoding. *Bioinformatics* **32**: 2920–2927.

Stark S, Egelkraut D, Aronsson KÅ, Olofsson J. 2019. Contrasting vegetation states do not diverge in soil organic matter storage: evidence from historical sites in tundra. *Ecology* **7**: e02731.

Steidinger BS, Crowther TW, Liang J, Van Nuland ME, Werner GDA, Reich PB, Nabuurs GJ, de Miguel S, Zhou M, Picard N *et al.* 2019. Climatic controls of decomposition drive the global biogeography of forest-tree symbioses. *Nature* **569**: 404–408.

Sterkenburg E, Bahr A, Brandström Durling M, Clemmensen KE, Lindahl BD. 2015. Changes in fungal communities along a boreal forest soil fertility gradient. *New Phytologist* **207**: 1145–1158.

Suz LM, Bidartondo MI, van der Linde S, Kuyper TW. 2021. Ectomycorrhizas and tipping points in forest ecosystems. *New Phytologist* **231**: 1700–1707.

Talbot JM, Allison SD, Treseder KK. 2008. Decomposers in disguise: mycorrhizal fungi as regulators of soil C dynamics in ecosystems under global change. *Functional Ecology* **22**: 955–963.

Tonjer L-R, Thoen E, Morgado L, Botnen S, Mundra S, Nybakken L, Bryn A, Kauserud H. 2021. Fungal community dynamics across a forest–alpine ecotone. *Molecular Ecology* **30**: 4926–4938.

Tourna M, Freitag TE, Nicol GW, Prosser JI. 2008. Growth, activity and temperature responses of ammonia-oxidizing archaea and bacteria in soil microcosms. *Environmental Microbiology* **10**: 1357–1364.

Ueda T, Suga Y, Yahiro N, Matsuguchi T. 1995. Remarkable N_2-fixing bacterial diversity detected in rice roots by molecular evolutionary analysis of nifH gene sequences. *Journal of Bacteriology* **177**: 1414–1417.

Van der Putten WH, Bardgett RD, Bever JD, Bezemer TM, Casper BB, Fukami T, Kardol P, Klironomos JN, Kulmatiski A, Schweitzer JA *et al.* 2013. Plant–soil feedbacks: the past, the present and future challenges. *Journal of Ecology* **101**: 265–276.

Ward EB, Duguid MC, Kuebbing SE, Lendemer JC, Bradford MA. 2022. The functional role of ericoid mycorrhizal plants and fungi on carbon and nitrogen dynamics in forests. *New Phytologist* **235**: 1701–1718.

Ward EB, Duguid MC, Kuebbing SE, Lendemer JC, Warren RJ, Bradford MA. 2021. Ericoid mycorrhizal shrubs alter the relationship between tree mycorrhizal dominance and soil carbon and nitrogen. *Journal of Ecology* **109**: 3524–3540.

Wardle DA. 2002. Communities and ecosystems: linking the aboveground and belowground components. In: Levin SA, Horn HS, eds. *Monographs in population biology, vol. 34.* Princeton, NJ, USA: Princeton University Press.

Wardle DA, Hornberg G, Zackrisson O, Kalela-Brundin M, Coomes DA. 2003. Long-term effects of wildfire on ecosystem properties across an Island area gradient. *Science* **300**: 972–975.

Welsh A, Chee-Sanford JC, Connor LM, Löffler FE, Sanford RA. 2014. Refined NrfA phylogeny improves PCR-based nrfA gene detection. *Applied and Environmental Microbiology* **80**: 2110–2119.

White TJ, Bruns T, Lee S, Taylor J. 1990. Amplification and direct sequencing of fungal ribosomal RNA genes for phylogenetics. In: Innis MA, Gelfand DH, Sninsky JJ, White TJ, eds. *PCR protocols: a guide to methods and applications.* San Diego, CA, USA: Academic Press, 315–322.

Ylänne H, Madsen RL, Castaño C, Metcalfe DB, Clemmensen KE. 2021. Reindeer control over subarctic treeline alters soil fungal communities with potential consequences for soil carbon storage. *Global Change Biology* **27**: 4254–4268.

Zhao M, Jones CM, Meijer J, Lundquist PO, Fransson P, Carlsson G, Hallin S. 2017. Intercropping affects genetic potential for inorganic nitrogen cycling by root-associated microorganisms in *Medicago sativa* and *Dactylis glomerata.* *Applied Soil Ecology* **119**: 260–266.

Zhu K, McCormack ML, Lankau RA, Egan JF, Wurzburger N. 2018. Association of ectomycorrhizal trees with high carbon-to-nitrogen ratio soils across temperate forests is driven by smaller nitrogen not larger carbon stocks. *Journal of Ecology* **106**: 524–535.

Supporting Information

Additional Supporting Information may be found online in the Supporting Information section at the end of the article.

Fig. S1 Geographical location of the sampled sites.

Fig. S2 Variation partitioning of the soil fungal community composition.

Fig. S3 Relative abundances of exploration types of ectomycorrhizal species in each vegetation type.

Fig. S4 Linear regressions between soil C : N ratios and microbial abundances.

Fig. S5 Soil C–N relationships along the heath and forest gradient.

Fig. S6 Canonical correspondence analysis of the fungal community composition, constrained by soil carbon and nitrogen.

Methods S1 Supplementary methods.

Table S1 Cycling conditions for quantitative PCRs.

Table S2 Differences in copy numbers of fungi (ITS), bacteria (16S) and functional genes and relative abundances of fungal functional groups.

Please note: Wiley is not responsible for the content or functionality of any Supporting Information supplied by the authors. Any queries (other than missing material) should be directed to the *New Phytologist* Central Office.

© 2022 The Authors
New Phytologist © 2022 New Phytologist Foundation

14698137, 2023, 6, Downloaded from https://nph.onlinelibrary.wiley.com/doi/10.1111/nph.18679 by Swedish University Of Agricultural Sciences, Wiley Online Library on [28/07/2023]. See the Terms and Conditions (https://onlinelibrary.wiley.com/terms-and-conditions) on Wiley Online Library for rules of use; OA articles are governed by the applicable Creative Commons License